ISSN 1063-7745, Crystallography Reports, 2006, Vol. 51, No. 3, pp. 357–365. © Pleiades Publishing, Inc., 2006.
Original Russian Text © A.I. Orlova, A.K. Koryttseva, E.V. Bortsova, S.V. Nagornova, G.N. Kazantsev, S.G. Samoilov, A.V. Bankrashkov, V.S. Kurazhkovskaya, 2006, published in Kristallografiya, 2006, Vol. 51, No. 3, pp. 391–399.

CRYSTAL CHEMISTRY

Crystallochemical Modeling, Synthesis, and Study of New Tantalum and Niobium Phosphates with a Framework Structure

A. I. Orlova[a], A. K. Koryttseva[a], E. V. Bortsova[a], S. V. Nagornova[a], G. N. Kazantsev[b], S. G. Samoilov[b], A. V. Bankrashkov[b], and V. S. Kurazhkovskaya[c]

[a] *Nizhni Novgorod State University, pr. Gagarina 23, Nizhni Novgorod, 603950 Russia*
e-mail:oai@unic.nnov.ru
[b] *Institute of Physics and Power Engineering, pl. Bondarenko 1, Obninsk, Kaluga oblast, 249033 Russia*
[c] *Moscow State University, Vorob'evy gory, Moscow, 119992 Russia*

Received June 20, 2005

Abstract—A crystallochemical approach is used to model the compositions of phosphates of pentavalent elements with the expected structure. New phosphates with a framework structure of the $T^{I}_{2}T^{III}_{3/2}T^{V}_{1/2}(PO_4)_3$ type (T^{I} = Na or K; T^{III} = Al, Cr, or Fe; and T^{V} = Nb or Ta) are synthesized and characterized by X-ray diffraction analysis (including high-temperature diffraction) and IR spectroscopy. It is established that, depending on the nature of the alkali cation (Na or K), these compounds are crystallized in two structural modifications: rhombohedral and cubic (sp. gr. $R\bar{3}c$ and $P2_13$, respectively). The unit-cell parameters and the thermal expansion coefficients of the phosphates under study are determined and the dependences of these characteristics on the nature of cations are established.

PACS numbers: 61.50.Ah

DOI: 10.1134/S1063774506030011

INTRODUCTION

Among mixed cation–anion frameworks, the most widespread are those composed of octahedra and tetrahedra. The general formula of such frameworks for phosphates can be written as $[T^{I}_{a}T^{II}_{b}T^{III}_{c}\ldots(PO_4)_3]^{n-}_{3\infty}$ where T^{I}, T^{II}, T^{III}, … are cations in the oxidation states from +1 to +5 in various combinations and ratios $a : b : c$: …; and n is the framework charge. The theoretically possible formula types for these frameworks were calculated by us previously [1] on the basis of the general principles of formation of mixed frameworks [2]. The calculations showed that more than half of these frameworks are formed by pentavalent elements in combination with mono-, di-, tri-, and tetravalent elements.

The role of pentavalent elements in the formation of such framework structures and development of new compounds as a basis of new materials has been studied by us and at other laboratories all over the world.

In recent years, the interest in such compounds has been related to the possibility of their participation in various chemical processes based on redox reactions (chemical and electrochemical intercalation, catalysis, etc.) [3–6]. In this case, pentavalent elements, exhibiting a larger number of oxidation states, have advantages over other elements.

The above-mentioned practical properties, in combination with the thermal, radiation, and chemical stability of phosphates of pentavalent elements, impel researchers to pay more attention to these compounds. It is expedient to search for new compounds within the structure–property–composition model, i.e., to use crystallochemical information as a basis for new synthesis studies [7].

In [8], we analyzed the structural data on the known phosphates of pentavalent elements, on the basis of which new phosphates with expected structural and thermal properties, in particular, extremely small and controlled thermal expansion, were "constructed." We synthesized and studied phosphates with electrically neutral ($n = 0$) and charged ($n = 1$) frameworks based on di- and pentavalent and tri-and pentavalent elements [9, 10].

In this study, the concept of directed synthesis is developed for phosphates with the framework charge $n > 1$. The purpose was to predict phosphates of new compositions, $T^{I}_{2}[T^{V}_{1/2}T^{III}_{3/2}(PO_4)_3]$ (T^{I} = Na or K; T^{V} = Nb or Ta; and T^{III} = Al, Cr, or Fe), with the framework charge $n = 2$ and expected rhombohedral and cubic

structures; to carry out their synthesis; to analyze the structure and morphotropy in isostoichiometric series of compounds; and to investigate regularities of their behavior upon heating.

A characteristic fragment of the frameworks of the rhombohedral and cubic modifications of $[T_2(PO_4)_3]$ is a dimer composed of two TO_6 octahedra linked by three bridge PO_4 tetrahedra. Aggregation of polyhedra into a 3D framework occurs in both cases by sharing terminal oxygen atoms of neighboring dimers. Individuality of the architectural motif of these structural types is determined by the mutual position of TO_6 and PO_4 polyhedra.

In the rhombohedral modification (the structural type $NaZr_2(PO_4)_3$ (NZP) of the mineral kosnarite), all dimers are oriented parallel to the single threefold axis and are located at the vertices and the center of an elementary rhombohedron. Thus, a rhombohedral cell belonging to the sp. gr. $R\bar{3}c$ is formed. In the cubic modification (the structural type of the mineral langbeinite), dimers are oriented in four directions along nonintersecting threefold axes parallel to the main diagonals of the cube. Thus, a cubic cell belonging to the sp. gr. $P2_13$ is formed.

The most significant consequence of the difference in the spatial arrangement of polyhedra is the number of cavities formed in the framework and their shape. In the rhombohedral modification, these cavities form four positions and the crystallochemical formula can be written as $(M1)^{[6]}(M2)_3^{[8]}[L_2^{[6]}(PO_4)_3]_{3\infty}$. In the cubic modification, the cavities form two positions and the crystallochemical formula has the form $(M1)^{[9]}(M2)^{[9]}[L_2^{[6]}(PO_4)_3]_{3\infty}$. $^{[6]}$, $^{[8]}$, and $^{[9]}$ are the coordination numbers of cation polyhedra in the corresponding positions.

Both rhombohedral and cubic modifications are observed in phosphates containing cations in the oxidation states from +4 to + 1 [1]. The phosphates of pentavalent elements have been observed only in the rhombohedral modification [8].

The knowledge of the above-mentioned crystallochemical peculiarities of rhombohedral and cubic structures makes it possible to construct phosphates in such structural modifications with new cation compositions. In this case, the empirical law [11] describing the effect of the limiting values of the difference Δr in the effective radii of the cations occupying framework and extraframework positions on the type of the framework structure (rhombohedral or cubic) is taken into account.

EXPERIMENTAL

The objects of study were the tantalum phosphates with trivalent elements, $Na_2Al_{3/2}Ta_{1/2}(PO_4)_3$, $Na_2Cr_{3/2}Ta_{1/2}(PO_4)_3$, $Na_2Fe_{3/2}Ta_{1/2}(PO_4)_3$, $K_2Al_{3/2}Ta_{1/2}(PO_4)_3$, $K_2Cr_{3/2}Ta_{1/2}(PO_4)_3$, and $K_2Fe_{3/2}Ta_{1/2}(PO_4)_3$, and isostoichiometric niobium phosphates, $Na_2Fe_{3/2}Nb_{1/2}(PO_4)_3$ and $K_2Fe_{3/2}Nb_{1/2}(PO_4)_3$.

The samples were obtained by solid-phase synthesis [10] performed in several stages. The starting reagents were Al_2O_3 (reagent grade), Cr_2O_3, Fe_2O_3, Ta_2O_5, Nb_2O_5 (reagent grade), $NaNO_3$ (reagent grade), KCl (reagent grade), and $NH_4H_2PO_4$ (reagent grade).

Tantalum oxide was obtained by burning shavings of metallic tantalum in air at 600 to 700°C. Chromium and iron oxides were prepared by the techniques described in [12]. To synthesize Fe_2O_3, 200 g of $FeCl_3 \cdot 6H_2O$ (analytical-purity grade) were dissolved in 1 l of distilled water and heated to 70°C. Then, 500 ml of 5-% solution of NH_4OH (analytic grade) was added to the solution obtained from a drop funnel with intense stirring. The resulting precipitate $Fe(OH)_3$ was washed on a Buchner funnel to a negative reaction of the washing water with NO^{3-} anions (diphenylamine test). The $Fe(OH)_3$ precipitate was dried at 110°C, then ground in an agate mortar, and calcined at 500°C for 5 h until Fe_2O_3 oxide was formed. Chromium oxide was obtained by decomposition of bichromate of ammonium according to the reaction $(NH_4)_2Cr_2O_7 \longrightarrow Cr_2O_3 + N_2 + 4H_2O$. The bichromate $(NH_4)_2Cr_2O_7$, ground into a powder, was placed in a large porcelain cup, some drops of ethyl alcohol were added, and the mixture obtained was fired. The thus prepared niobium, tantalum, iron, and chromium oxides were identified by X-ray diffraction.

Then, the above-mentioned reagents, taken in a stoichiometric ratio, were ground in an agate mortar and heated in air at 450°C for 4 h. As a result, the ammonium dihydrophosphate decomposed and the gaseous reaction products were removed. Then the mixture was isothermally annealed in air at temperatures of 600, 700, 800, 900, and 1000°C for 24–36 h in each stage. Intermediate monitoring of the phase formation was performed by X-ray powder diffraction. Each heating stage was alternated with dispersion.

The samples of phosphates obtained were investigated by X-ray diffraction (including high-temperature diffraction) and IR spectroscopy. X-ray diffraction patterns of phosphates were recorded on a DRON-3.0 diffractometer using CuK_α filtered radiation (λ = 1.54178 Å) at room temperature in the 2θ angle range from 11° to 50°. The error in measuring angles did not exceed 0.015° (the corresponding errors in determining the lattice parameter of the samples studied were of 0.005 Å along the *a* axis and 0.01 Å along the *c* axis). The IR spectra of the compounds under study were recorded on a SPECORD-75IR spectrophotometer in the wave number range from 1400 to 400 cm^{-1}. The samples for spectral analysis were finely dispersed

Table 1. The unit-cell parameters of $Na_2T^{III}_{3/2}T^{V}_{1/2}(PO_4)_3$ and $K_2T^{III}_{3/2}T^{V}_{1/2}(PO_4)_3$ phosphates (T^{III} = Al, Cr, or Fe; T^{V} = Nb or Ta)

Compound	a, Å	c, Å	V, Å^3	Compound	a, Å	V, Å^3
$Na_2Al_{3/2}Ta_{1/2}(PO_4)_3$	8.460(5)	21.77(1)	1349(3)	$K_2Al_{3/2}Ta_{1/2}(PO_4)_3$	9.726(2)	920(1)
$Na_2Cr_{3/2}Ta_{1/2}(PO_4)_3$	8.587(5)	21.95(1)	1401(3)	$K_2Cr_{3/2}Ta_{1/2}(PO_4)_3$	9.831(5)	949(1)
$Na_2Fe_{3/2}Ta_{1/2}(PO_4)_3$	8.655(5)	21.91(1)	1421(3)	$K_2Fe_{3/2}Ta_{1/2}(PO_4)_3$	9.909(2)	973(1)
$Na_2Fe_{3/2}Nb_{1/2}(PO_4)_3$	8.654(5)	21.91(1)	1421(3)	$K_2Fe_{3/2}Nb_{1/2}(PO_4)_3$	9.909(2)	973(1)

Note: Sodium phosphates: rhombohedral cell, sp. gr. $R\bar{3}c$; potassium phosphates: cubic cell, sp. gr. $P2_13$.

Table 2. Thermal expansion parameters of $Na_2T^{III}_{3/2}T^{V}_{1/2}(PO_4)_3$ and $K_2T^{III}_{3/2}T^{V}_{1/2}(PO_4)_3$ phosphates (T^{III} = Al, Cr, or Fe; T^{V} = Nb or Ta)

Compound	$\alpha_a \times 10^6$, °C^{-1}	$\alpha_c \times 10^6$, °C^{-1}	$\alpha_{av} \times 10^6$, °C^{-1}	$\lvert\alpha_a - \alpha_c\rvert \times 10^6$, °C^{-1}	Compound	$\alpha_a \times 10^6$, °C^{-1}
$Na_2Al_{3/2}Ta_{1/2}(PO_4)_3$	1.0[a]	17.0[a]	6.3	16.0	$K_2Al_{3/2}Ta_{1/2}(PO_4)_3$	7.4[c]
$Na_2Cr_{3/2}Ta_{1/2}(PO_4)_3$	−0.2[a]	20.4[a]	6.7	20.6	$K_2Cr_{3/2}Ta_{1/2}(PO_4)_3$	6.8[a]
$Na_2Fe_{3/2}Ta_{1/2}(PO_4)_3$	−0.4[a]	23.9[a]	7.7	24.3	$K_2Fe_{3/2}Ta_{1/2}(PO_4)_3$	6.9[b]
$Na_2Fe_{3/2}Nb_{1/2}(PO_4)_3$	1.0[a]	25.7[a]	9.2	24.7	$K_2Fe_{3/2}Nb_{1/2}(PO_4)_3$	8.0[c]

Note: Sodium phosphates: rhombohedral cell, sp. gr. $R\bar{3}c$; potassium phosphates: cubic cell, sp. gr. $P2_13$.
[a] 25–630°C.
[b] 25–690°C.
[c] 25–730°C.

films prepared by deposing a suspension in isopropyl alcohol on a KBr substrate with subsequent drying.

The behavior of phosphates upon heating was studied on a DRON-3M diffractometer (CuK_α filtered radiation) with a high-temperature attachment URVT-1500. The thermal expansion coefficients were determined from the shift of the diffraction peaks from the crystallographic planes [*hkl*] with the use of the technique described in [13]. Temperature was measured with a Pt–Pt/10%Rh thermocouple.

RESULTS AND DISCUSSION

The compounds synthesized were crystalline powders. Aluminum-, chromium-, and iron-containing compounds were, respectively, colorless, green, and beige with a pink tint.

The X-ray powder data suggest that the formation of crystalline products occurred at 800–900°C. A further increase in temperature to 1000°C led to an increase in the intensity of reflections.

Depending on the nature of the alkali element (Na or K), as was expected, two groups of X-ray diffraction patterns were observed. The X-ray diffraction patterns of sodium phosphates (Fig. 1a) were similar in the position and relative intensity of the diffraction peaks. As an analog for their indexing, we chose the phosphate $NbTi(PO_4)_3$, crystallizing in a rhombohedral cell, sp. gr. $R\bar{3}c$, and belonging to the NZP structural type [5]. In turn, the X-ray diffraction patterns of potassium phosphates were also similar to each other (Fig. 1b) but differed from the diffraction patterns of sodium phosphates. Indexing was performed using as an analog langbeinite $K_2Mg_2(SO_4)_3$, which crystallizes in a cubic cell, sp. gr. $P2_13$ [14]. The X-ray diffraction patterns of some phosphates showed additional weak reflections.

The results of indexing were used to calculate the unit-cell parameters of the new compounds (Tables 1, 2).

The samples of the phosphates prepared, assigned to the rhombohedral and cubic structural modifications in accordance with the X-ray diffraction data, were also characterized by IR spectroscopy.

Figure 2a shows the IR spectra of sodium-containing orthophosphates of trivalent elements (Fe, Cr, and Al), Ta, and Nb. Figure 2b demonstrates the spectra of potassium-containing orthophosphates of the same elements. The general formula of these orthophosphates is $T^{I}_2[T^{V}_{1/2}T^{III}_{3/2}(PO_4)_3]$. The spectra are similar owing to the similarity of the structural types to which the compounds under consideration belong. In the range 1100

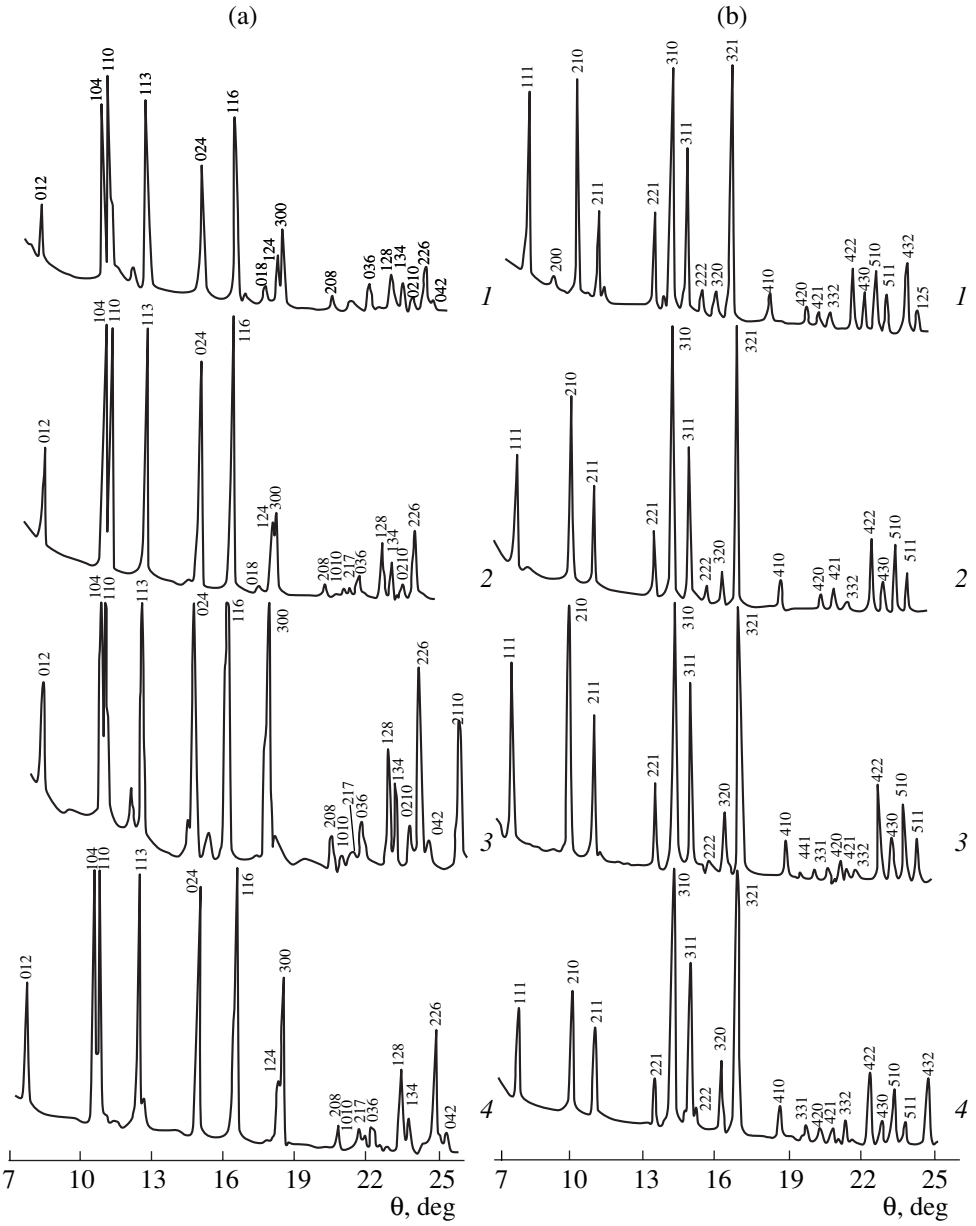

Fig. 1. X-ray diffraction patterns of (a) sodium phosphates (*1*) $Na_2Al_{3/2}Ta_{1/2}(PO_4)_3$, (*2*) $Na_2Cr_{3/2}Ta_{1/2}(PO_4)_3$, (*3*) $Na_2Fe_{3/2}Ta_{1/2}(PO_4)_3$, and (*4*) $Na_2Fe_{3/2}Nb_{1/2}(PO_4)_3$ and (b) potassium phosphates (*1*) $K_2Al_{3/2}Ta_{1/2}(PO_4)_3$, (*2*) $K_2Cr_{3/2}Ta_{1/2}(PO_4)_3$, (*3*) $K_2Fe_{3/2}Ta_{1/2}(PO_4)_3$, and (*4*) $K_2Fe_{3/2}Nb_{1/2}(PO_4)_3$.

to 900 cm^{-1}, stretching vibrations of the tetrahedral PO_4 ion manifest themselves. In the range 650 to 450 cm^{-1}, bending vibrations of this ion are observed. In the NZP (sp. gr. $R\bar{3}c$) and langbeinite (sp. gr. $P2_13$) structures, the positional symmetry of the PO_4 tetrahedron is reduced to C_2 and C_1, respectively.

The factor-group analysis of the vibrations of PO_4 tetrahedra with the positional symmetry C_2 in the sp. gr. $R\bar{3}c$ (the factor group D_{3d}) allows the occurrence of up to five bands of asymmetric stretching (ν_3) and asymmetric bending (ν_4) vibrations, one band of symmetric stretching vibrations ν_1, and two bands of symmetric bending vibrations ν_2 in the spectrum [15]. In Fig. 2a (curves *2–4*), closely located bands of asymmetric stretching vibrations ν_3 overlap each other and, as a result, one wide band peaked at ~1100 cm^{-1} is observed in the spectrum. In the spectrum of the $Na_2Al_{3/2}Ta_{1/2}(PO_4)_3$ phosphate (Fig. 2a, curve *1*), this wide band is split into five maxima, allowed by the selection rules. The band at ~900 cm^{-1} corresponds to symmetric stretching vibrations ν_1. In the region of

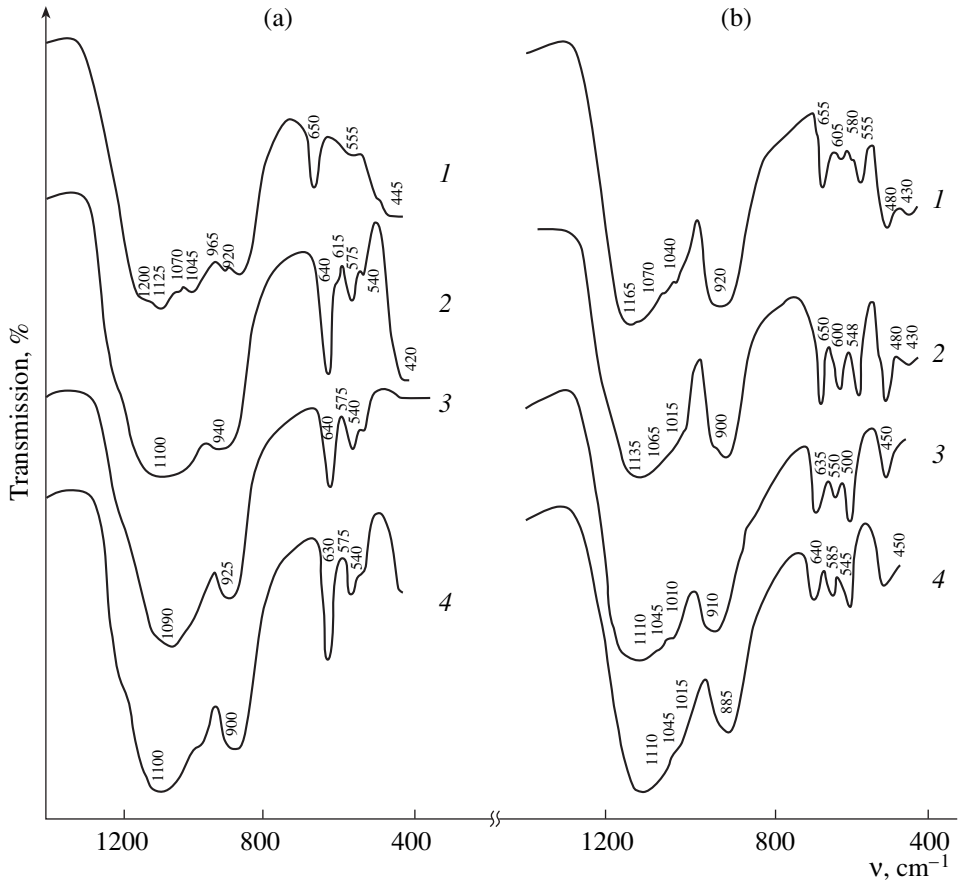

Fig. 2. IR spectra of (a) sodium phosphates (*1*) $Na_2Al_{3/2}Ta_{1/2}(PO_4)_3$, (*2*) $Na_2Cr_{3/2}Ta_{1/2}(PO_4)_3$, (*3*) $Na_2Fe_{3/2}Ta_{1/2}(PO_4)_3$, and (*4*) $Na_2Fe_{3/2}Nb_{1/2}(PO_4)_3$ and (b) potassium phosphates (*1*) $K_2Al_{3/2}Ta_{1/2}(PO_4)_3$, (*2*) $K_2Cr_{3/2}Ta_{1/2}(PO_4)_3$, (*3*) $K_2Fe_{3/2}Ta_{1/2}(PO_4)_3$ and (*4*) $K_2Fe_{3/2}Nb_{1/2}(PO_4)_3$.

bending vibrations ν_4 (640–540 cm^{-1}), three or four bands from those five allowed by the selection rules manifest themselves. Bending vibrations ν_2 are represented by the band in the range near 400 cm^{-1}. The second, lower-frequency band of vibrations ν_2 cannot be detected with the measuring system we used.

According to the factor-group analysis of the vibrations of the tetrahedral ion with the positional C_1 symmetry in the sp. gr. $P2_13$ (the factor group *T*), the spectrum should contain three bands of vibrations ν_3, three bands of vibrations ν_4, one band of vibrations ν_1, and two bands of vibrations ν_2 [16]. In Fig. 2b (curves *1*, *2*), two more bands (or shoulders) due to vibrations ν_3 of the PO_4 ion are observed on the low-frequency slope of the wide band at ~1110 cm^{-1}. This peculiarity is one of the differences of the spectra from those of the NZP phases. In the spectra of aluminum- and chromium-containing phosphates $Na_2Al_{3/2}Ta_{1/2}(PO_4)_3$ and $Na_2Cr_{3/2}Ta_{1/2}(PO_4)_3$, the bands of asymmetric stretching vibrations ν_3 are blue-shifted (to 1165 cm^{-1}) owing to the smaller sizes of Al and Cr cations (Fig. 2b, curves *1*, *2*). The band at ~900 cm^{-1}, as well as in the previous series, corresponds to the symmetric stretching vibrations ν_1 of the P–O bond. In the region of asymmetric bending vibrations ν_4, a triplet of bands of approximately equal intensity is observed, which is characteristic of the IR spectrum of compounds with the langbeinite structure. In the spectrum of the $K_2Al_{3/2}Ta_{1/2}(PO_4)_3$ phosphate, the central band of the triplet is divided into two weak bands, one of which may correspond to vibrations of the Al–O bond. The spectrum of the potassium phases in this region differs significantly from the spectra of compounds with NZP structure. The band at 450 cm^{-1} in Fig. 2b (curves *3*, *4*) corresponds to vibrations ν_2. In the spectra of the aluminum- and chromium-containing phosphates $K_2Al_{3/2}Ta_{1/2}(PO_4)_3$ and $K_2Cr_{3/2}Ta_{1/2}(PO_4)_3$, the bending-vibration bands, as well as the stretching-vibration bands, are blue-shifted. As a result, both bands of bending vibrations ν_2 at 480 and 430 cm^{-1} are observed in these spectra.

Thus, the results of IR spectral analysis are in agreement with the X-ray diffraction data and indicate the crystallization of the sodium and potassium phosphates of trivalent elements (Fe, Cr, Al), Ta, and Nb with the

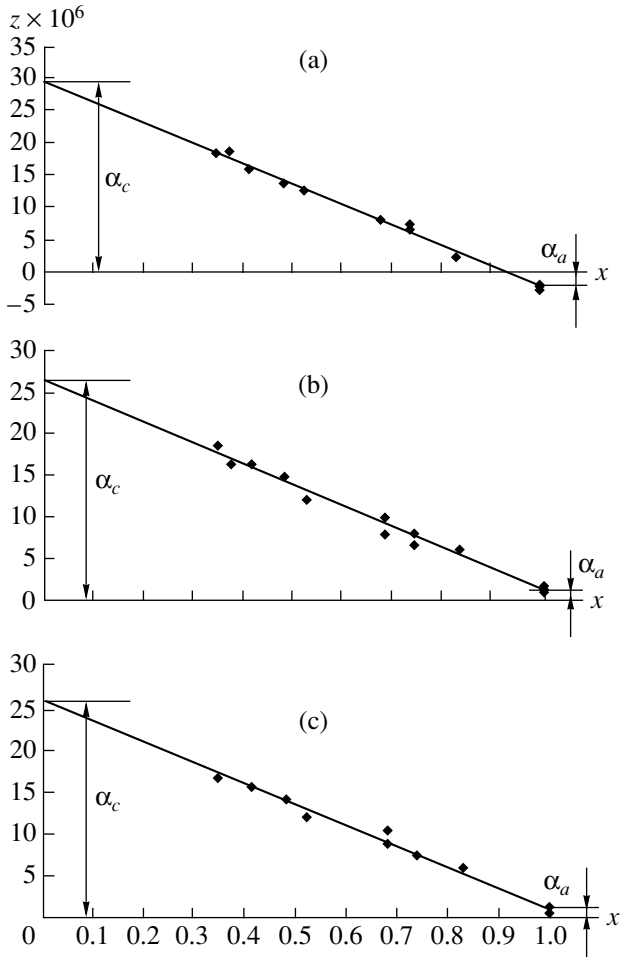

Fig. 3. Dependences $z = f(x_i)$ for the $Na_2Fe_{3/2}Nb_{1/2}(PO_4)_3$ phosphate at t = (a) 200, (b) 400, and (c) 600°C; α_a and α_c were determined according to [13].

general formula $T_2^{\mathrm{I}}T_{3/2}^{\mathrm{III}}T_{1/2}^{\mathrm{V}}(PO_4)_3$ in different structural types (NZP and langbeinite).

The IR spectral and X-ray diffraction data obtained in this study allowed us to analyze the effect of the nature (radius, electronic structure, and polarizing ability) of trivalent and pentavalent cations on the crystallographic characteristics of the compounds under consideration.

As was expected, according to the crystallochemical prediction, the morphotropic transition NZP ⟶ langbeinite was observed when we passed from potassium to sodium containing compounds. The unit-cell parameters of the rhombohedral phase (a and c) and the cubic phase (a) increase only slightly with increasing trivalent cation radius [17] and almost do not change when niobium is replaced by tantalum (owing to the equality of their ionic radii; see Tables 1, 2).

The changes in the phosphate structure upon heating were evaluated from the thermal expansion coefficients, which were calculated from the high-temperature X-ray diffraction data obtained in the temperature range from 20 to 80°C. For the phosphates with NZP structure (sp. gr. $R\bar{3}c$), we measured the thermal displacements $\Delta\theta$ of the crystallographic planes (104), (110), (113), (204), (116), (300), (306), (218), (226), (21.10), (410), (31.10), and (416); for the phosphates with a cubic lattice, the displacements of the (111), (210), (211), (221), (310), (311), (321), (422), (510), (520), and (611) were measured. An example of the calculation of the thermal expansion parameters by the technique described in [13], using the graphical dependences $z = f(x_i)$, is shown in Fig. 3 (here, $z = -\dfrac{\Delta\theta_i \cot(\Delta\theta_i)}{\Delta T_i}$ and x_i is a characteristic depending on the indexes of the planes and the unit-cell parameters; the equation for calculating x_i was reported in [13]). The thermal expansion coefficients α_a, α_c, and $\alpha_{av} = (2\alpha_a/3 + \alpha_c/3)$ for the phosphates with hexagonal and cubic structures are listed in Table 2. It is obvious from these data that the sodium phosphates $Na_2Al_{3/2}Ta_{1/2}(PO_4)_3$, $Na_2Cr_{3/2}Ta_{1/2}(PO_4)_3$, $Na_2Fe_{3/2}Ta_{1/2}(PO_4)_3$, and $Na_2Fe_{3/2}Nb_{1/2}(PO_4)_3$ and the potassium phosphates $K_2Al_{3/2}Ta_{1/2}(PO_4)_3$, $K_2Cr_{3/2}Ta_{1/2}(PO_4)_3$, $K_2Fe_{3/2}Ta_{1/2}(PO_4)_3$, and $K_2Fe_{3/2}Nb_{1/2}(PO_4)_3$ behave differently upon heating.

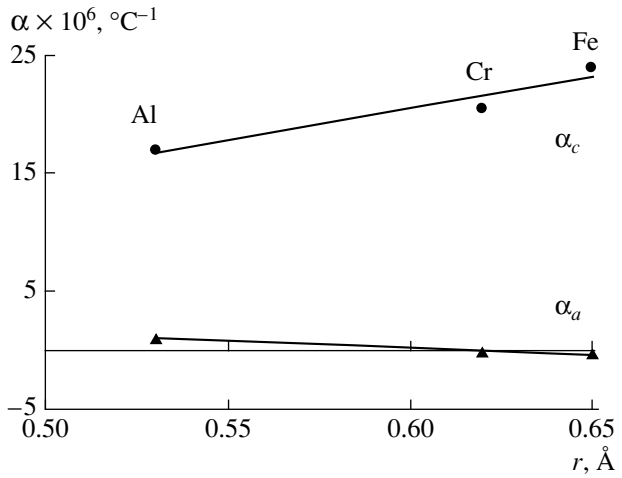

Fig. 4. Dependences of α_a and α_c on the radius r of the trivalent Al, Cr, and Fe cations.

The sodium phosphates expand anisotropically (this behavior is characteristic of phosphates of the NZP family [18]): the parameter α_c increases ($\alpha_c > 0$), whereas α_a either decreases ($\alpha_a < 0$) or slightly increases ($|\alpha_a| \approx 0$).

With an increase in the radius of framework cations, α_c increases, whereas α_a slightly decreases (Fig. 4).

The found values of the thermal expansion coefficients of rhombohedral phosphates allowed us to determine also the changes in the rhombohedron parameters

(the edge length l and the angle β between the edges) upon heating (Table 3). The values of l and β were calculated from the equations [19]

$$l = a/3\sqrt{3 + (c/a)^2}; \quad b = 1.5/\sqrt{3 + (c/a)^2}.$$

The dependences of their changes $\Delta l/l$ and Δβ on the trivalent cation radius upon heating in the temperature range under study (Fig. 5) indicate that the contribution of $\Delta l/l$ and Δβ to the thermal lattice strain changes when we pass from aluminum to chromium and from chromium to iron. In the first case (the radius of the T^{III} cation is 0.53–0.62 Å), the lattice strain results from the increase in the rhombohedron edge length l with a simultaneous decrease in the angle β. In this second case, the lattice strain is due to the increase in the edge length, whereas the angle β remains almost constant.

The character of the dependences of α_a, α_c, $\Delta l/l$, and Δβ on the nature of the trivalent cation (in particular, its radius), established here, is in agreement with that reported in [20] for the NZP-type phosphates containing titanium, zirconium, or hafnium framework cations ($NaTi_2(PO_4)_3$, $NaZr_2(PO_4)_3$, and $NaHf_2(PO_4)_3$). As was shown in [20], this character can also be due to the effect of the polarizing ability of the corresponding cations, which decreases when we pass from titanium to hafnium and zirconium and from aluminum to chromium and iron. In this case, the localization of the electron density at the P–O(T^{III}) bond increases when we pass from iron to aluminum (with decreasing ionic radius); accordingly, the bond force also increases in this series. As a result, the thermal rotation of $T^{III}O_6$ octahedra and PO_4 tetrahedra (according to the model of thermal expansion described in [18]) is more hindered.

Apparently, this effect is one of the reasons for the lowest thermal strain in the aluminum-containing compound $Na_2Al_{3/2}Ta_{1/2}(PO_4)_3$ among those studied here (Table 2).

Such a character of the change in the force of the P–O bond in the series of the phosphates under consideration is in agreement with their IR spectra. Indeed, with increasing force of the P–O(T^{III}) bond in the series T^{III} = Fe, Cr, and Al, which is due to the increase in the polarizing ability of T^{III} cations, the absorption band of asymmetric vibrations ν_3 of the phosphate group shifts to higher frequencies: 1090 cm^{-1} (Fe), 1100 cm^{-1} (Cr), and 1200 cm^{-1} (Al).

Table 3. Rhombohedron parameters for $Na_2T^{III}_{3/2}T^{V}_{1/2}(PO_4)_3$ phosphates (T^{III} = Al, Cr, or Fe; T^{V} = Nb or Ta) in the temperature range 25–630°C

Compound	l, Å	$\Delta l/l \times 10^{-3}$	β, deg	Δβ, deg
$Na_2Al_{3/2}Ta_{1/2}(PO_4)_3$	8.813	7.5	57.41	−0.43
$Na_2Cr_{3/2}Ta_{1/2}(PO_4)_3$	8.912	8.4	57.59	−0.54
$Na_2Fe_{3/2}Ta_{1/2}(PO_4)_3$	8.934	9.6	57.93	−0.62
$Na_2Fe_{3/2}Nb_{1/2}(PO_4)_3$	8.944	11.0	57.90	−0.65

It is also noteworthy that the cell parameters a and c of the isostoichiometric tantalum ($Na_2Fe_{3/2}Ta_{1/2}(PO_4)_3$) and niobium ($Na_2Fe_{3/2}Nb_{1/2}(PO_4)_3$) phosphates are the same (owing to the equality of the ionic radii of Nb and Ta) (Table 1), whereas the thermal expansion coefficients of niobium phosphates are always somewhat larger (Table 2). This phenomenon can be explained by the lower electron density of the P–O(Nb) bond in comparison with the P–O(Ta) bond due to the corresponding difference in the polarizing abilities of niobium and tantalum. (Apparently, since this difference is small, it did not manifest itself in the IR spectra.)

In contrast to the rhombohedral phosphates of the NZP family (sodium-containing compounds), the potassium phosphates $K_2Al_{3/2}Ta_{1/2}(PO_4)_3$, $K_2Cr_{3/2}Ta_{1/2}(PO_4)_3$, $K_2Fe_{3/2}Ta_{1/2}(PO_4)_3$, and $K_2Fe_{3/2}Nb_{1/2}(PO_4)_3$ (cubic cell, langbeinite type, sp. gr. $P2_13$), according to the results of our investigation,

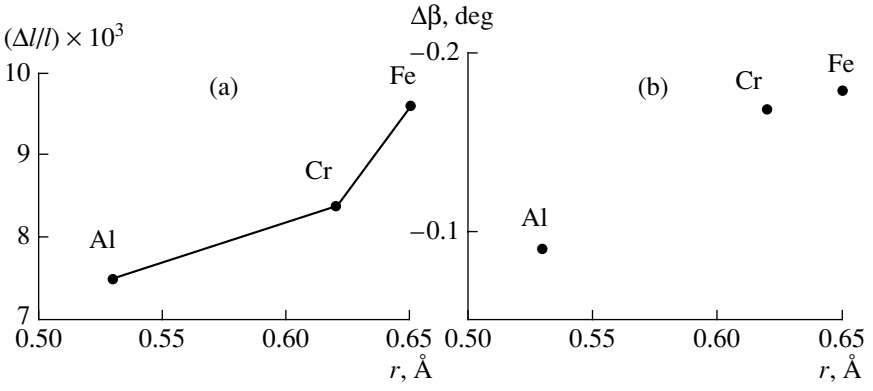

Fig. 5. Dependences of the heating-induced (a) relative change $\Delta l/l$ in the rhombohedron edge length and (b) change Δβ in the rhombohedron angle on the radius r of the trivalent framework-forming cations Al, Cr, or Fe.

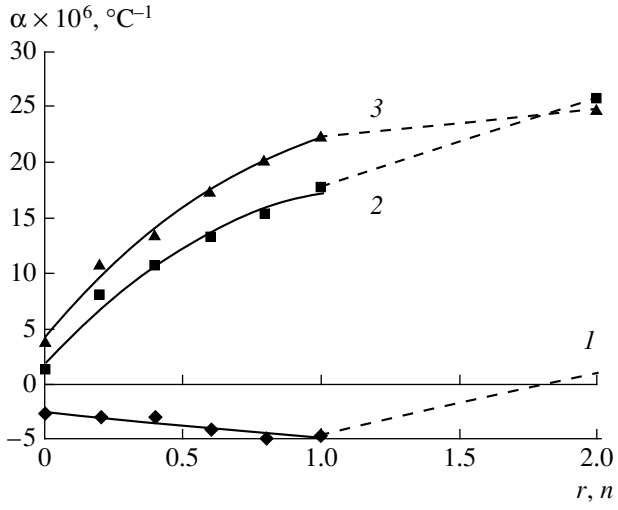

Fig. 6. Dependences of (*1*) α_a, (*2*) α_c, and (*3*) the anisotropy $|\alpha_a - \alpha_c|$ on the charge n of the $[Fe_{1/2+x}Nb_{3/2-x}(PO_4)_3]^{n-}$ framework in the series of $Na_{2x}[Fe_{1/2+x}Nb_{3/2-x}(PO_4)_3]$ phosphates ($0 \le n \le 2$, $n = 2x$).

expand isotropically upon heating. A similar character of thermal expansion was also observed previously for other phosphates of this modification ($K_2Mg_{3/2}Zr_{1/2}(PO_4)_3$ and $Cs_2Mg_{3/2}Zr_{1/2}(PO_4)_3$ [21, 22]).

The new experimental data obtained in this study and previously [23] allowed us to reveal the general trend of the change in the thermal expansion characteristics in series of niobium phosphates with frameworks of the $[Fe_{1/2+x}Nb_{3/2-x}(PO_4)_3]^{n-}$ type with a change in the framework charge n from zero to two ($0 \le n \le 2$) and the corresponding changes in x from zero to unity ($0 \le x \le 1$).

The dependences of α_a, α_c, and $|\alpha_a - \alpha_c|$ on n (Fig. 6) for the compounds from the $Na_{2x}Fe_{1/2+x}Nb_{3/2-x}(PO_4)_3$ series indicate the following:

(i) At $n = 0$ and $x = 0$, α_a and α_c are close to zero and the expansion anisotropy $|\alpha_a - \alpha_c|$ is also close to zero (all M positions are vacant).

(ii) With an increase in n in the range $0 \le n \le 1$ and x in the range $0 \le x \le 0.5$, the anisotropy increases (this behavior is characteristic of NZP compounds) with increasing expansion (compression) along the c (a) axis; in this case, filling of $M1$ positions occurs from completely vacant (at $n = 0$) to completely occupied (at $n = 1$) positions.

(iii) With an increase in n and x in the ranges $1 \le n \le 2$ and $0.5 \le x \le 1$, respectively, the parameter α_c continues to increase (although with smaller $d\alpha_c/dn$), whereas the curve $\alpha_a = f(n)$ shows an inflection at $n \approx 1$ and the compression decreases to almost zero ($M2$ positions are also occupied).

The dependences of α_a, α_c, and $|\alpha_a - \alpha_c|$ on the framework charge n (and, obviously, the occupancy of M positions) for the phosphates with T^V and T^{III} cations (by the example of the series of $Na_{2x}Fe_{1/2+x}Nb_{3/2-x}(PO_4)_3$ phosphates ($0 \le x \le 1$)) (Fig. 6) are in good correspondence with the similar dependences for the phosphates with T^{IV} and T^{III} cations (by the only known example of the series of $Na_xY_{x-1}Zr_{3-x}(PO_4)_3$ phosphates ($1.5 \le x \le 2$) [24]). Additional investigations are necessary to confirm the empirical regularity revealed by the example of these two series.

The results obtained in this study have confirmed the correctness of the crystallochemical prediction about the existence of phosphates of pentavalent elements with the calculated chemical compositions $T^I_2T^{III}_{3/2}T^V_{1/2}(PO_4)_3$, specified structure (rhombohedral and cubic modifications), and expected behavior upon heating.

ACKNOWLEDGMENTS

This study was supported by the Russian Foundation for Basic Research (project no. 05-03-32127) and the Ministry of Education and the Ministry of Industry, Science, and Technology of the Russian Federation (Subprogram no. 3, "Development of the Infrastructure of Scientific–Technical and Innovation Activity of the Highest School and Its Personnel Potential"; Section no. 3.3, "Development of the Research Work of Young Teachers and Researchers, Postgraduate Students, and Students").

REFERENCES

1. A. I. Orlova, Radiokhimiya **44** (5), 385 (2002).
2. A. A. Voronkov, V. V. Ilyukhin, and N. V. Belov, Kristallografiya **20** (3), 556 (1975) [Sov. Phys. Crystallogr. **20**, 340 (1975)].
3. D. A. Stratiĭchuk, V. V. Lesnyak, M. S. Slobodyanik, and N. V. Stus', Zh. Neorg. Khim. **46** (9), 1449 (2001).
4. A. K. Padhi, K. S. Nanjundaswamy, C. Masquelier, and J. B. Goodenough, J. Electrochem. Soc. **144** (8), 2581 (1997).
5. F. J. Berry, C. Greaves, and J. F. Marko, J. Solid State Chem. **96**, 408 (1992).
6. M. Manickam, J. Power Sources **113**, 179 (2003).
7. B. I. Lazoryak, Usp. Khim. **65** (4), 307 (1996).
8. A. I. Orlova and A. K. Koryttseva, Kristallografiya **49** (5), 811 (2004) [Crystallogr. Rep. **49**, 724 (2004)].
9. A. I. Orlova, V. I. Pet'kov, M. V. Zharinova, et al., Zh. Prikl. Khim. **76** (1), 14 (2003).
10. M. V. Zharinova, A. I. Orlova, A. K. Koryttseva, et al., Zh. Neorg. Khim. **49** (2), 174 (2004).
11. A. I. Orlova, V. A. Orlova, A. V. Buchirin, et al., Radiokhimiya **47** (3), 203 (2005).
12. Yu. V. Karyakin and I. I. Angelov, *Pure Chemical Materials* (Khimiya, Moscow, 1974) [in Russian].

13. S. G. Samoĭlov, A. I. Orlova, G. N. Kazantsev, and A. V. Bankrashkov, Kristallografiya **51** (3), 519 (2006).
14. A. Zeman and J. Zeman, Acta Crystallogr. **10**, 409 (1957).
15. V. S. Kurazhkovskaya, Zh. Strukt. Khim. **41** (1), 74 (2000).
16. A. I. Orlova, I. G. Trubach, V. S. Kurazhkovskaya, et al., J. Solid State Chem. **173**, 314 (2003).
17. R. D. Shannon, Acta Cristallogr. A **32**, 751 (1976).
18. J. Alamo, J. Solid State Ionic **63–65**, 547 (1993).
19. S. G. Samoĭlov, A. I. Kryukova, and G. N. Kazantsev, Neorg. Mater. **28** (10/11), 2197 (1992).
20. K. V. Govindan Kutty, R. Asuvathraman, C. K. Mathews, and U. V. Varadaraju, Mater. Res. Bull. **29** (10), 1009 (1994).
21. A. I. Orlova, V. A. Orlova, A. V. Buchirin, et al., Radiokhimiya **47** (3), 213 (2005).
22. V. A. Orlova, in *Proceedings of the IX Annual Scientific and Practical Conference of Young Researchers, 2004, Nizhni Novgorod* (NGTU, Nizhni Novgorod, 2004), p. 52.
23. M. V. Zharinova, A. I. Orlova, A. K. Koryttseva, et al., Zh. Neorg. Khim. **49** (2), 174 (2004).
24. O. Toshitaka and Y. Iwao, J. Am. Ceram. Soc. **69** (1), 1 (1986).

Translated by Yu. Sin'kov